A Plug-and-Play Ripple Mitigation Approach for DC-Links in Hybrid Systems

Sinan Li[1], Albert T. L. Lee[1], Siew-Chong-Tan[1] and S. Y. (Ron) Hui[1,2]
Email: snli@eee.hku.hk, tlalee@eee.hku.hk, sctan@eee.hku.hk, ronhui@eee.hku.hk
[1]Department of Electrical and Electronic Engineering, The University of Hong Kong, Hong Kong, China
[2]Department of Electrical and Electronic Engineering, Imperial College London, U.K.

***Abstract*—In this paper, a plug-and-play ripple mitigation technique is proposed. It requires only the sensing of the DC-link voltage and can operate fully independently to remove the low-frequency voltage ripple. The proposed technique is non-intrusive to the existing hardware and enables hot-swap operation without disrupting the normal functionality of the existing power system. It is user-friendly, modular and suitable for plug-and-play operation. The experimental results demonstrate the effectiveness of the ripple-mitigation capability of the proposed device. The DC-link voltage ripple in a 110 W miniature hybrid system comprising an AC/DC converter and two resistive loads is shown to be significantly reduced from 61 V to only 3.3 V. Moreover, it is shown that with the proposed device, the system reliability has been improved by alleviating the components' thermal stresses.**

***Keywords*—Plug-and-play ripple mitigation, ripple pacifier, DC-link, AC/DC power system.**

I. INTRODUCTION

In recent years, with the rapid penetration of distributed renewable energy sources (such as solar photovoltaic, wind power) into the traditional AC power network, it is envisaged that a mixture of AC power grids and emerging DC power grid will emerge as a future form of power network. A typical infrastructure of a hybrid power grid is shown Fig. 1(a), where power conversions such as AC/DC, DC/AC and DC/DC link the various AC and DC power sources/loads together. In the system, the electrical energy is transmitted and distributed through an intermediate DC voltage link. A stable and reliable operation of DC-link is of vital importance because a large variation of the DC-link voltage can lead to efficiency and performance degradation of its upstream/downstream converters, increased voltage stresses of the system and coupled interference between the DC and AC utilities [1], [2]. For specific applications, the DC-link voltage fluctuation will generate flickers in the LED lightings [3], [4], shorten the life expectancy of a battery in electric vehicle applications [5], [6], and reduce the power efficiency in the PV panels [7], [8] and fuel cells [9]. Large voltage ripple across the electrolytic capacitors (E-caps) also leads to significant capacitor current ripple and thus internal resistive loss and temperature rise inside the E-Cap.

With the growing use of low-power-rating single-phase AC/DC converters, such as the plug-in AC modules for PV applications [10], one critical challenge with the DC-link in an AC-DC hybrid system is that the it suffers from a steady-state oscillation with a double-line frequency component (i.e. 100 Hz or 120 Hz for a 50 Hz or 60 Hz grid, respectively). The oscillation is caused by the instantaneous power difference between the AC and DC side in single-phase AC/DC converters [1], [2]: at the AC side, power will be varying at double-line frequency around a DC offset; while at the DC side, a constant power is desired. To buffer the power imbalance and stabilize the DC-link voltage, large and bulky capacitors must be installed in parallel with the DC-link either dispersedly over the transmission and distribution line or locally near the source/load converters (as the ones

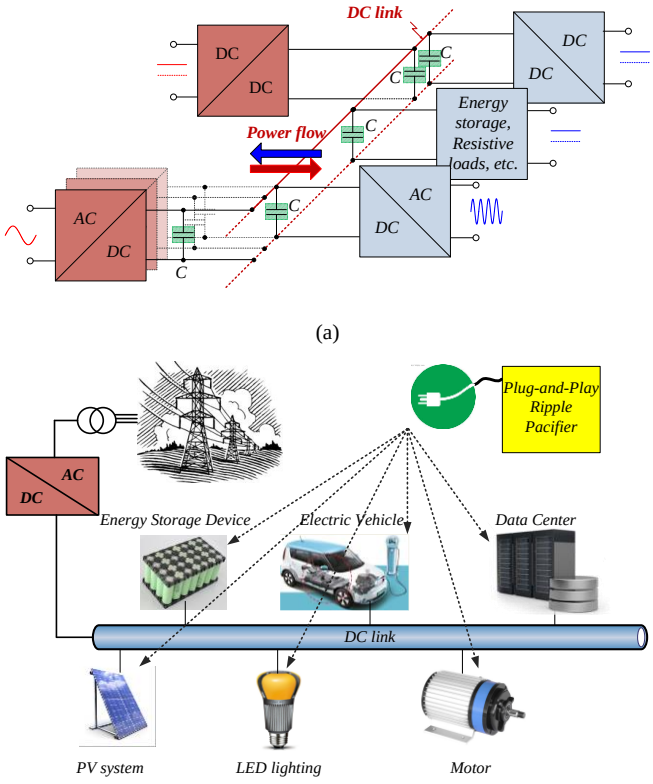

Fig. 1. (a) Typical power stage infrastructure of power electronic systems with an intermediate DC-link; (b) overview of the proposed plug-and-play ripple mitigation scheme for the DC-link in a hybrid power systems.

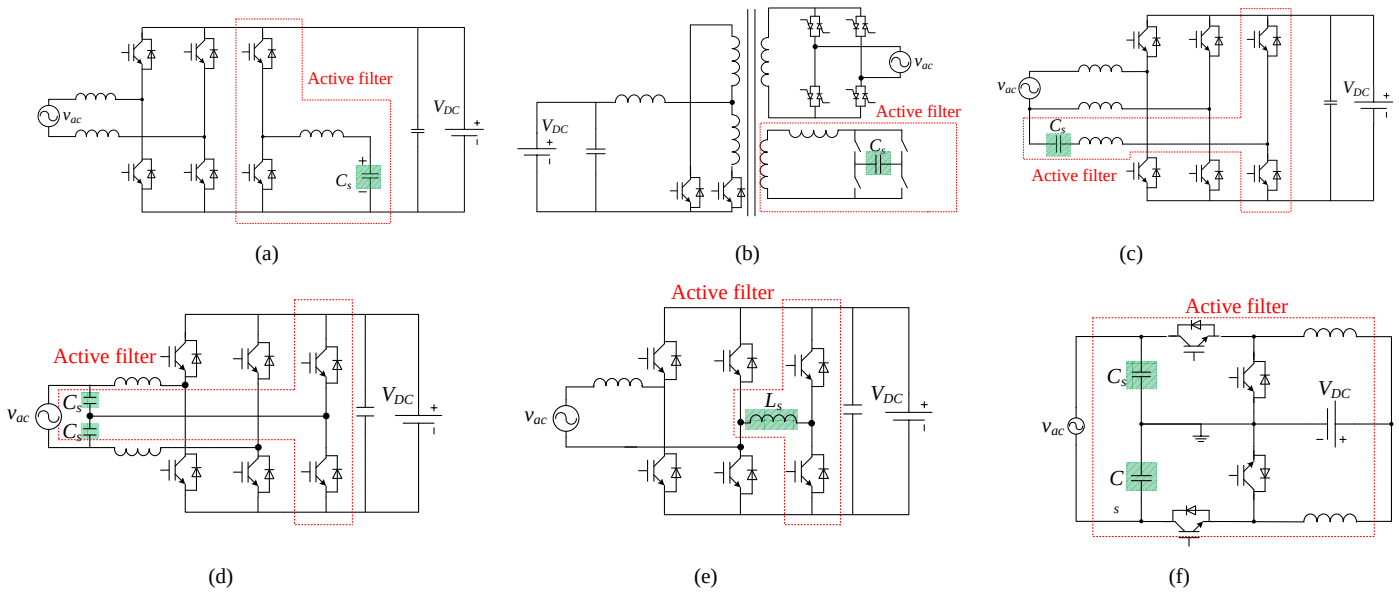

Fig. 2. Various circuit diagrams for implementing an active-filter with an AC/DC converter.

shown in Fig. 1(a) and labeled as C). Typically, E-caps are common selections of DC-link capacitors due to their space-saving and cost-effective nature. However, their high failure rates substantially undermine the system's reliability [5]–[8], [11], [12]. Their limited lifetime is also highly incompatible with that of existing renewable technologies. It is reported that a typical E-cap has a lifetime of merely 1000–7000 hours at 105 $^{\circ}C$, and the number is halved with each additional 10 $^{\circ}C$ rise in the junction temperature [13]–[15]. In contrast, PV is reported to have a life expectancy of more than 20 years [16], [17]. A recent trend to tackle the reliability issue is to eliminate the use of E-caps with active-power-filter-based approaches. The principles of operation are to store the ripple power in a separate energy storage component and to allow a large voltage/current fluctuation across it. In this way, small but long lifetime film capacitors can be used to stabilize the DC-link voltage with enhanced system reliability. Another benefit of this approach is that the volume of the switching converters in the host system can be significantly shrunk with the removal of the relatively large E-caps [18].

Despite the advantages of the active-filter-based approach, the installation and maintenance of an active filter can be a tedious task. As will be reviewed in Section II, the prior arts solutions typically require modifications and re-design of the existing host system before an active filter can be used. This inevitably increases the cost of the overall systems at both power supplies' and demands' ends. In this paper, a new concept called plug-and-play ripple mitigation is proposed. It is physically realized as a two terminal device, whose major objective is to achieve DC-link voltage stabilization based on the active-filter concept, but it differentiates itself from prior arts with a distinctive feature of hot-swap operation, i.e., tdevice can be easily attached and detached on-line from the DC-link. Therefore, the device requires no modification of its host DC system and can operate as a stand-alone equipment. The proposed approach includes a device known as the plug-and-play ripple pacifier (RP), as shown in Fig. 1(b). It can simply be plugged into the DC-link distributedly and/or locally. For example, it can be installed locally on the PV side of an AC inverter module for the purpose of power decoupling. In the event that the proposed device breaks down and fails to operate, it can be swapped out with a new one in a plug-and-play manner. The success of the device largely relies on (i) the selection of a proper power electronics topology and (ii) the proposed DC-ripple-based control techniques. Importantly, by performing the small-signal analysis, the device is shown to be non-intrusive to the normal operation of the DC power system. The effectiveness of the ripple-mitigating function, the non-intrusive property of the RP and viability of hot-swapping operation are experimentally verified in a 110 W miniature AC-DC hybrid system.

II. Existing Active-Filter-Based Approaches

A. Hardware

The circuit configurations of an active filter with the existing host systems can be manipulated in several ways. It can be (i) a complete switching converter that can work independently (Fig. 2(a) and (b)), (ii) a semi-complete switching converter which can only operate normally by sharing some of the components with the host systems (Fig. 2(c)–(e)), and (iii) a fully integrated switching converter that shares all the components with the host systems (Fig. 2(f)). The energy storage components in these active filters can be a capacitor (Fig. 2 (a)–(d), (f)), an inductor (Fig. 2(e)) or batteries, with bipolar or unipolar operating waveforms.

Of these active filter configurations, the integrated solution (Fig. 2(f)) achieves active filtering by modifying the operation waveforms in the original host converters which potentially increases the current/voltage stress. Therefore, the original hardware, including its controllers, must be re-designed. For the combined solution (e.g. Fig. 2(c), (e) and (f)), no modification of the existing system is necessary. However, these active filters require the access of several terminals of the host system, e.g. the AC side, the DC side and/or the phase leg switches, and thus a hot-swap installation of such an active filter is difficult. For the solution which employs a complete switching converter, there might still be problems with the installation. For instance, in Fig. 2(b), a complete re-design of the high-frequency transformer is required. This is because the active filter is magnetically coupled to the host system, and the energy storage requirement of the high-frequency transformer can be different from that in the original designs.

B. *Sensing and Control*

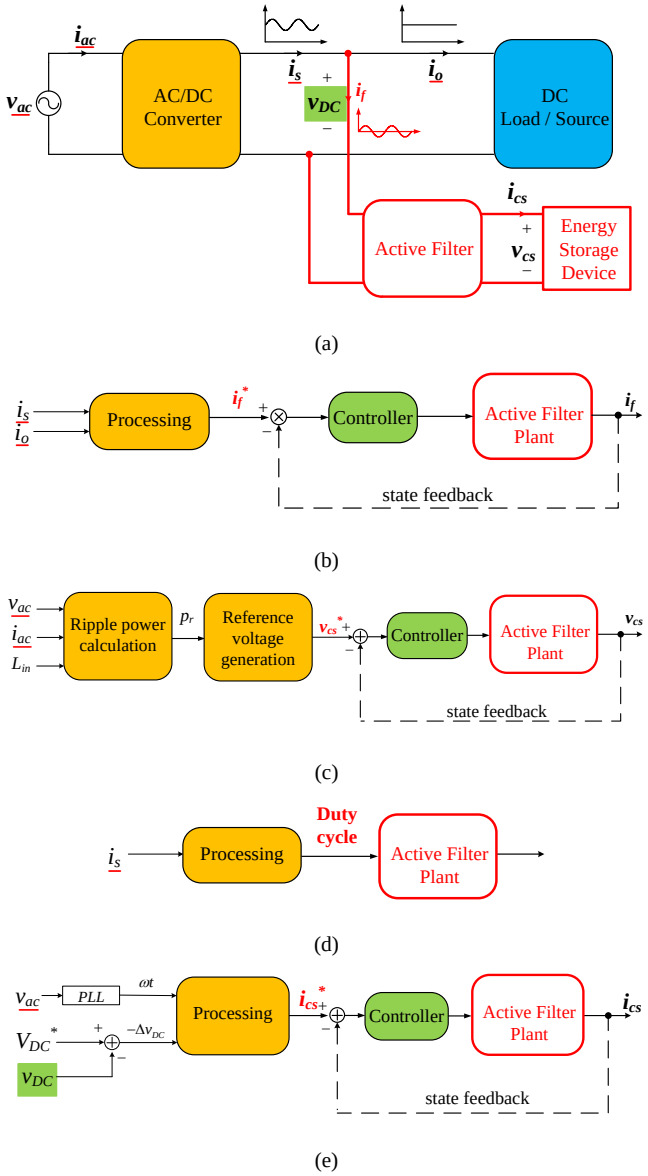

Fig. 3. (a) A simplified schematics of a DC system with active filter and (b–e) existing control methods for an active filter used in a DC system.

The implementation of sensing and control in an active filter can also prohibit a true plug-and-play operation of the ripple mitigation. This can be explained using a simplified schematic in Fig. 3(a), where a single-phase AC/DC converter, a DC load/ source (converter) and a shunt active filter are included. It should be noted that all the configurations in Fig. 2 can be equivalently translated into Fig. 3(a). Assuming a constant DC-link voltage v_{DC}, the DC-link current from the AC/DC converter i_s will contain a DC and a double-line frequency content. By introducing a compensation current i_f into the DC-link, the shunt device can eliminate the low-frequency oscillations in the DC-link, leading to an stable DC current i_o for the DC load/source. The compensation current i_f from the shunt active filter can be controlled directly or indirectly. To date, there are four basic methods to control the active filter, as illustrated in Fig. 3(b)–(e), and they are described in more detail as follows.

(i) Direct control of i_f in a closed-loop such that it follows a reference signal i_f^*, as shown in Fig. 3(b). Since i_f should only compensate the AC component of the DC-link current i_s, the derivation of i_f^* often involves the measurement of i_s. For instance, i_f^* can be obtained by calculating $i_f^* = i_s - I_o$, where I_o is the DC portion of i_o [19]. In [11], [20]–[23], a high-pass filter, a neural filter and a virtual-capacitor-based control is applied to i_s to exact the AC component .

(ii) Direct control of the instantaneous power in the energy storage device in a closed-loop, such that it matches the ripple power generated by the AC/DC converter, as shown in Fig. 3(c). Such a method involves an estimation of the ripple power from the AC/DC stage and a reference generation algorithm for the energy storage device to track. To estimate the ripple power, a measurement of v_{ac} and i_{ac} is needed. To obtain a more accurate result, the values of the internal inductors, capacitors and power loss in the host systems must be known [7], [24].

(iii) Direct calculation of the required duty cycle based on the AC component in the DC-link current i_s, as shown in Fig. 3(c) [18], [25].

(iv) Direct regulation of the instantaneous DC-link voltage v_{DC} in a closed-loop, as shown in Fig. 3(e). However, the measurement of v_{ac} is still required to provide phase information for the active filter reference generation [26].

With reference to the four control methods, it is worth noting that direct measurements of variables such as the DC-link current i_s, the DC load current i_o or the AC side current/ voltage/ phase information is required. Since implementing a current sensor requires opening the AC line or the DC-link, and the AC voltage sensing is typically achieved far away from the local point of connection of an active filter, the requirements of these measurements render these methods unsuitable for plug-and-play operation. In a more practical system, where multiple AC and DC sources/loads are interconnected, collecting all the necessary information to formulate a proper reference command for the active filter will be a costly and inconvenient task.

III. Requirements for Being a True Plug-and-Play Device

Based on the review in Section II, to enable the true plug-and-playable feature, two requirements must be satisfied. First, the hardware of the device must be a complete switching converter and connected directly with the DC-link without intermediate coupling or connections, as shown in Fig. 4(a). Second, the controller must also be DC-link based which means that the only measurement required is the local DC-link voltage v_{DC} at the point of connection, as depicted in Fig. 4(b). Unlike previous methods, the proposed control scheme does *not* need to measure any voltage or current information (v_{ac}, i_{ac}, i_s) from the AC side or the current information (i_o) from the DC side. In addition, it does not require a priori knowledge of the exact system parameters used in the existing system. Moreover, the method is local-information-based which does *not* require any communications between the various AC and DC sources/loads. In this paper, an active filter with a plug-and-play ripple mitigation feature is referred to as a plug-and-play ripple pacifier (RP).

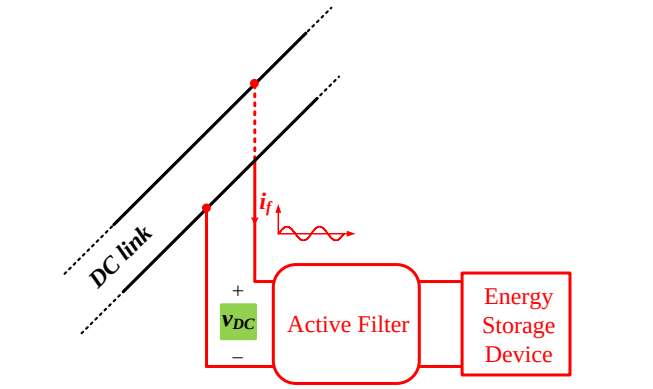

(a)

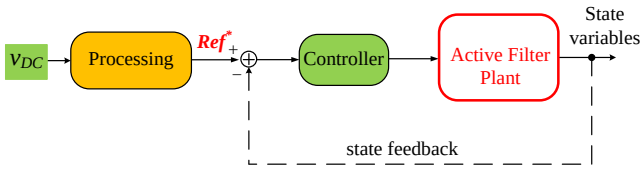

(b)

Fig. 4. Requirements for plug-and-play operation, namely (a) a shunt connection must exist on the DC port of the PFC rectifier and (b) the DC-link voltage v_{DC} is the only information required for the controller.

IV. Implementations of a Plug-And-Play Ripple Pacifier

A. Hardware configuration

An RP deals with AC ripple power only, and thus the switching converter must support bidirectional power conversion. Since the input of the RP is the DC-link voltage, while the output is connected to an energy storage device, whose voltage waveform can either be DC or AC, there is a myriad of DC-voltage-sourced topologies for selection, including at least step-down (forward) converter, step-up (boost) converter, step-up/down (flyback) converter and their combinations. Some of these converters can be constructed with a half-bridge or a full-bridge configuration. Switched capacitor converters are also possible candidates [27]. For very high voltage or power application, multilevel power converter can also be used if necessary.

With respect to the voltage level of the target DC-link voltage, there are mainly three rules which governs the circuit topology selection of an RP as follows.

a) The energy utilization rate of the energy storage should be large.

b) The size and cost of the energy storage device should be small.

c) High voltage stresses should be avoided.

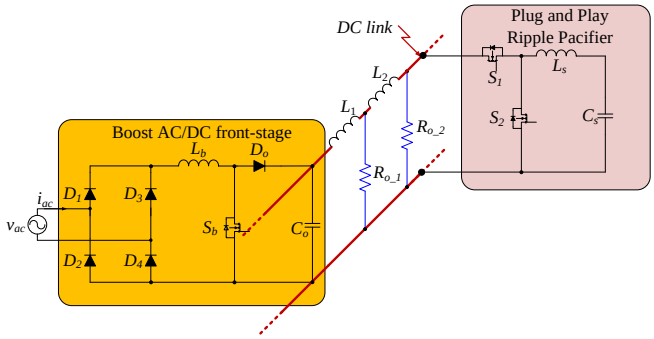

Fig. 5. Ideal circuit model of a boost-type PFC rectifier with a buck-type RP.

This paper focuses on a hybrid system with a high voltage DC-link as shown in Fig. 5, where a boost PFC rectifier is employed as the front-end stage of the DC-link with an average output voltage of V_{DC} = 400 V, and two resistive loads R_{o1} and R_{o2} are used to emulate the practical loading conditions with intermediate transmission impedance L_1 and L_2. A bi-directional buck-type RP with a capacitive energy storage C_s is selected and plugged into the DC-voltage link at the point of common coupling (PCC) near the load R_{o2}. Also, there is a pre-installed DC-link capacitor C_o, whose effective capacitance is deliberately chosen to be small enough to mimic the effect of aging and heating of the liquidated chemical contained in the E-Caps .

B. DC-Ripple-Based Control Techniques

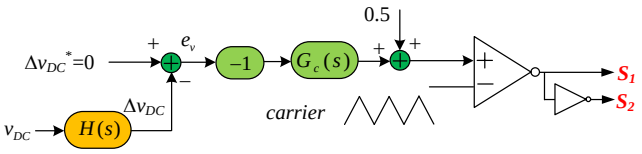

Fig. 6. Schematic diagram of the proposed ripple-voltage-based control method for the plug-and-play RP.

Fig. 6 illustrates the proposed DC-ripple-based control scheme, where the only requisite information is v_{DC}. The motivation is that the DC-link voltage ripple is caused by the unbalanced input and output power that flows into and out of the DC-link capacitor C_o, and that the DC-link voltage ripple

alone should contain sufficient information to predict the unbalanced ripple power p_r or the ripple current in i_s. In Fig. 6, the ripple voltage Δv_{DC} is initially obtained from v_{DC} through H(s), e.g. a high-pass filter, and then tightly regulated following a reference $\Delta v_{DC}^*=0$ through the closed-loop feedback control, thereby realizing zero voltage ripple on the DC-link. A feed-forward term of 0.5 is added to the final modulation signal such that the voltage across C_s will contain a $V_{DC}/2$ offset. It should be emphasized that albeit the proposed DC-ripple-based control appears to be simple and straightforward, it is the first control method reported that is suitable for a true plug and play operation.

C. Small-Signal Analysis

To facilitate the small-signal analysis of the RP with the proposed control schemes, an equivalent circuit diagram of Fig. 5 is obtained in Fig. 7(a). The transmission inductances have been neglected to ease the analysis and demonstrate the proof-of-concept. The current source i_s containing a DC and a double-line frequency component represents the AC/DC converter; the resistor R_o represents the total load on the DC voltage link, and r_p is the equivalent series resistance (ESR) in L_s and C_s. By performing state-space averaging and linearization of the model in Fig. 7(a), the small-signal control block diagram of the RP system can be obtained in Fig. 7(b), where G_{im}(s) is the RP plant transfer function from the duty cycle m to the average input current i_{S1}, as

$$G_{im}(s)=\frac{\langle i_{S1}\rangle(s)}{m(s)}=\frac{sC_sMV_{DC}}{s^2C_sL_s+sC_sr_p+1}, \qquad (1)$$

where $\langle\cdot\rangle$ is an averaging operator over a switching period, and the symbol ~ denotes small-signal perturbations. M is the steady-state value of the duty cycle m.

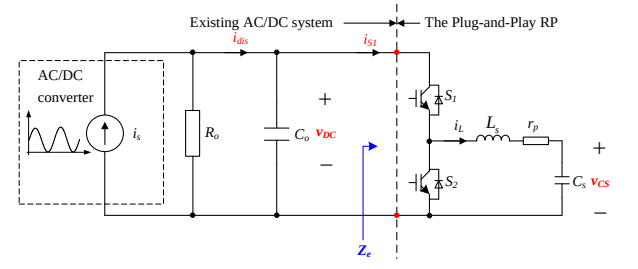

(a)

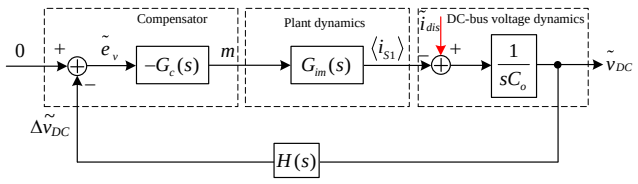

(b)

Fig. 7. (a) Equivalent circuit diagram of Fig. 5 and (b) The small-signal control block diagram of the RP system based on the linearized model.

From Fig. 7(b), the total open-loop gain $\ell(s)$ and the closed-loop $\tilde{v}_{DC}$ are given by (2) and (3) respectively as

$$\ell(s)=\frac{1}{sC_o}G_c(s)G_{im}(s)H(s). \qquad (2)$$

$$\tilde{v}_{DC}(s)=\frac{1}{sC_o\left[\ell(s)+1\right]}\tilde{i}_{dis}(s), \qquad (3)$$

In other words, to suppress the ripples in v_{DC}, $\ell(s)$ should be designed to have a high enough gain at frequencies with respect to $\tilde{i}_{dis}(s)$. A proportional-resonant (PR) controller whose resonant poles are designed precisely at the double-line frequency can be selected for the compensator G_c(s). To further complement the ripple mitigating performance, multi-RP controllers or repetitive controllers can be used for reducing high order ripples.

It is interesting to examine the impact of the RP to the host system by examining the input impedance Z_e of the RP, as defined in Fig. 7(a). Based on Fig. 7(b), Z_e can be derived in (4) whose Bode plots are shown in Fig. 8.

$$Z_e(s)=\frac{\tilde{v}_{DC}(s)}{\langle i_{S1}\rangle(s)}=\frac{1}{H(s)G_c(s)G_{im}(s)}=\frac{1}{s\left[C_o\ell(s)\right]} \qquad (4)$$

The zero impedance of the RP at 100 Hz exemplifies the ripple-mitigating capability of the RP from a filter point of view: any 100 Hz ripple power will be directly shorted to ground without going to the DC load. Meanwhile, the infinitely large impedance at low frequency (including DC) implies that the RP behaves like an open-circuit, so that adding the RP in parallel with the DC-link has negligible, if not zero, influence on the DC voltage regulation in the host AC/DC converter(s). Therefore, it can be concluded that applying an RP on the DC-link will only suppress the designated low-frequency ripple, and will not interfere with the existing AC/DC system.

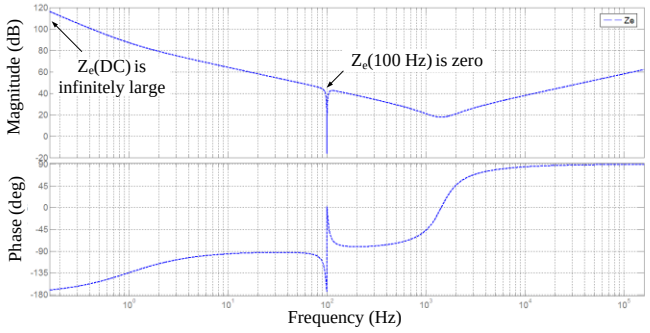

Fig. 8. Bode plots of the input impedance Z_e of the RP with a proportional-resonant controller whose resonant poles are set at 100 Hz.

V. Experiment Verifications

The effectiveness of the proposed plug-and-play ripple reduction scheme is experimentally verified in a system as that given in Fig. 5. Table I summarizes the key circuit parameters used for the experimental setup. Note that the pre-installed DC-link capacitor C_o has a small capacitance of merely 5 μF. Based on the power ratings of the loads which is 100 W, the energy storage capacitor C_s can be chosen as 5

μF to minimize the required energy storage. In a system with medium power ratings, a larger C_s should be utilized. For a high power system, multiple RPs with relative small C_s may be connected to the system in a distributive manner to operate simultaneously.

TABLE I. KEY CIRCUIT PARAMETERS FOR EXPERIMENTAL SETUP

Plug-and-Play RP Parameters	Values	Host System Parameters	Values
Input voltage V_{DC} (V)	400	**Nominal power P_{DC} (W)**	100
Energy storage capacitor C_s (μF)	5	**AC voltage v_{ac} (V)**	220
Inductor L_s (mH)	2.5	**Output voltage V_{DC} (V)**	400
Switching frequency f_{s1} (kHz)	25	**Dc-link capacitor C_o (μF)**	5
		ESR of C_o @ 400 V (Ω)	3.51
		Boost inductor L_b (μH)	390
		Load 1: R_{o_1} (Ω)	8000
		Load 2: R_{o_2} (Ω)	2000

A. *Steady-State Ripple Mitigation Performance*

Fig. 9 show the measured steady-state DC-link voltage waveforms before and after the proposed plug-and-play ripple mitigation device is applied to the DC-link.

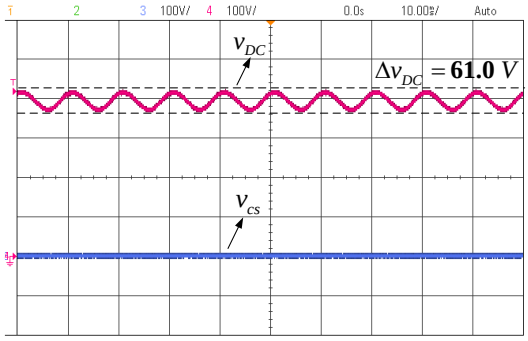

(a)

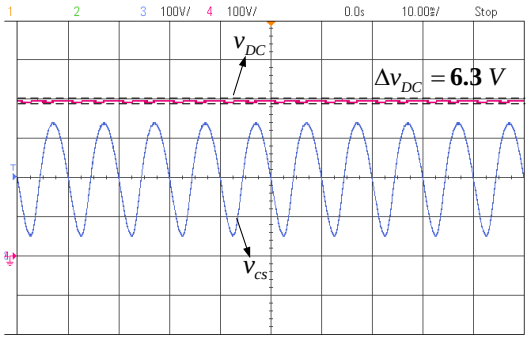

(b)

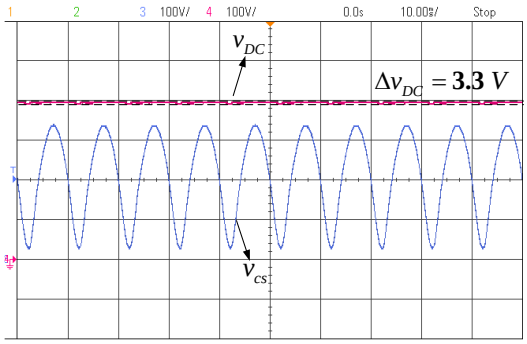

(c)

Fig. 9. Steady-state voltage waveforms of the DC-link and the energy storage capacitor with and without the plug-and-play ripple pacifier. (a) Without the ripple pacifier; (b) With the ripple pacifier (using a single PR controller resonant at 100 Hz); (c) With the ripple pacifier (using multiple PR controllers resonant at 100 Hz, 200 Hz, and 300 Hz).

Fig. 9(a) shows that before the RP is applied, there is a significant 100 Hz ripple in the v_{DC}. The measured peak-to-peak DC-link voltage ripple is 61 V, which accounts for 15.25% of the average DC-link voltage. The large ripple is mainly due to the a small capacitor C_o used on the DC-link. When the plug-and-play RP is activated and compensating at 100 Hz (through a single PR controller with a pair of resonant poles at 100 Hz), the DC-link voltage ripple is significantly mitigated from 61 V to 6.3 V, as shown in Fig. 9(b). At the same time, the voltage across C_s is pulsating significantly at 100 Hz between zero and v_{DC}. Since only a single PR controller is used, the capacitor voltage v_{cs} has a smooth and sinusoidal waveform. To further mitigate the high frequency ripples, multiple PR controllers (with resonant poles at 100 Hz, 200 Hz and 300 Hz) are used in a third experiment and the plug-and-play device is able to compensate ripples at 100 Hz, 200 Hz and 300 Hz. The measured v_{DC} is shown in Fig. 9(c) with a ripple of merely 3.3 V. With a multiple PR controller, a much sharper waveform is observed around the valley of v_{cs}, as compared with that in Fig. 9(b). The results in Fig. 9 successfully confirms the ripple mitigation capability with the proposed DC-ripple-based control techniques.

B. *Non-Invasive Property During Load Transient and Steady-State*

To demonstrate the non-invasive property of the RP, transient performance of the RP are examined, with four sets of step load change experiments (from full load to 20% load and from 20% load to full load) with and without the RP. The change of load power is realized by switching on and off the load R_{o_2} (80 W). The transient waveforms for the DC-link and the energy storage capacitor are shown in Fig. 10 and Fig. 11.

In both sets of experiments, the DC-link voltage with and without a plug-and-play RP has similar dynamics in terms of the overshoot/undershoot ratio and settling time during the load change transient. Meanwhile, during steady-state, the DC-link voltage is unchanged before and after the load transient. These observations verify the non-invasive

property of the proposed RP to the host system in regulating the average DC-bus voltage.

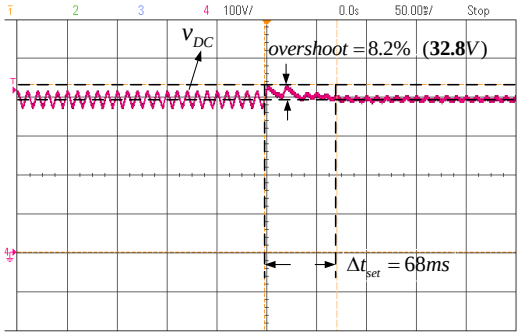

(a)

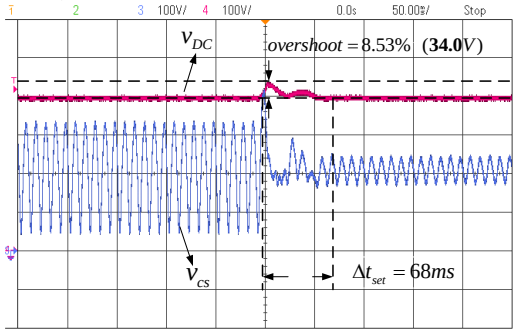

(b)

Fig. 10. Transient voltage waveforms from full load to 20% load (a) without the plug-and-play RP (b) with the plug-and-play RP.

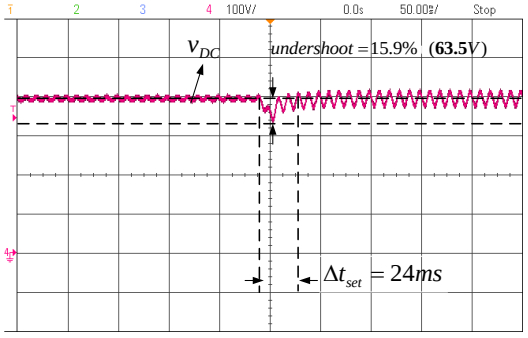

(a)

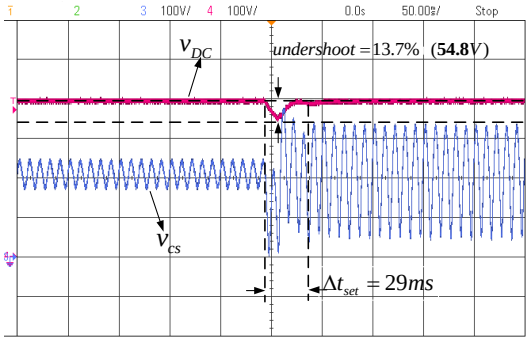

(b)

Fig. 11. Transient voltage waveforms from 20% load to full load (a) without the plug-and-play RP (b) with the plug-and-play RP.

C. *Hot-Swapping with Soft-Start*

To avoid undesired transient caused by the inrush current when the RP is activated or hot-swapped into the DC-link, a soft start function must be incorporated into the RP with a proper powering sequence. Fig. 12 illustrates the waveforms of v_{DC} and v_{cs} during the plug-in interval of an RP to the DC-link. At the plugged-in instant, the RP detects the connection with the DC-link and gradually increases the duty cycle of from zero to 50 %. In this way, v_{cs} is softly charged to half of the DC-link voltage, which is also the steady-state voltage of v_{cs}. No severe overshoot/undershoot or oscillations is observed in v_{DC}. The controller in the RP will be activated as soon as the soft-start ends. An immediate reduction of Δv_{DC} will then be obtained.

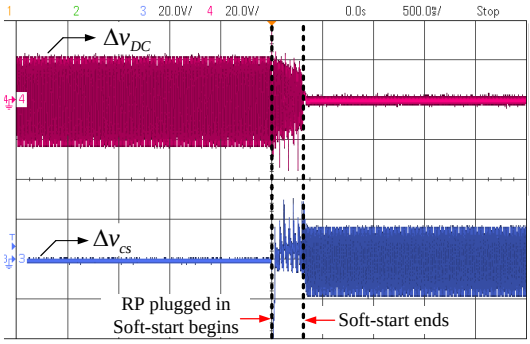

Fig. 12. Voltage waveforms of the DC-link ripple Δv_{DC} and energy storage ripple Δv_{cs} during hot-swapping interval of an RP.

D. *Theraml and Reliability Improvement of the Hybrid System*

By eliminating the ripple current inside the DC-link capacitor and ensuring a stable DC-link voltage, the junction temperature of C_o as well as that in the power devices and magnetics in the host AC/DC converters are expected to decrease.

TABLE II. MEASURED TEMPERATURE WITH AND WITHOUT RP

Measured Surface	Without RP (°C)	With RP (°C)	Temperature reduction ΔT (°C)
Plastic cover of E-Cap C_o	42.5	35.0	7.5
Aluminum top of E-Cap C_o	42.2	34.1	8.1
Output diode D_o	50.7	41.4	9.3
Power MOSFET S_b	42.4	33.9	8.5
Input diode bridge D_1~D_4	60.0	52.3	7.7
Magnetic core of L_b	64.7	54.3	10.4

Table II shows the experimentally measured surface temperatures of the boost PFC rectifier front stage taken after three hours of continuous operation under free convection at the ambient temperature of 25.4℃ with and without the use of RP. The measurement is conducted using thermal couplers and a FLUKE data acquisition unit. As expected, with the use of RP, all the power devices, magnetics, and the output E-cap have much lower temperatures than those without RP. The surface (junction) temperature of all the components has reduced by more than 7.5℃ which improves the operating lifetime of components and hence the reliability of the whole system. For instance, according to [13], [28], a 8.1 °C reduction of the surface temperature of an E-cap could extend its lifetime by 1.75 times.

VI. Conclusions

In this paper, a plug-and-play ripple mitigation technique for stabilizing the DC-link voltage is proposed. The major benefits of the proposed solution are that it is simple to use, cost-effective, modular in structure, and non-invasive to the existing AC/DC power system. Also, the capacitor on the DC bus can be made significantly smaller than that required in conventional AC/DC systems without the proposed auxiliary ripple energy storage. Longer lifetime film capacitors with lower equivalent series resistance (ESR) can therefore be used to replace the short-lifetime E-caps with high ESR. The experimental results confirm the effectiveness of the ripple-reduction capability of the proposed plug-and-play RP device on a boost-type PFC rectification system.

Acknowledgment

This work is supported by the Hong Kong Research Grant Council under the Theme-based project T22-715/12N.

References

[1] H. Wang and F. Blaabjerg, "Reliability of capacitors for dc-link applications in power electronic converters—an overview," *IEEE Trans. Ind. Appl.*, vol. 50, no. 5, pp. 3569–3578, Sep. 2014.

[2] L. Gu, X. Ruan, M. Xu, and K. Yao, "Means of eliminating electrolytic capacitor in AC/DC power supplies for LED lightings," *IEEE Trans. Power Electron.*, vol. 24, no. 5, pp. 1399–1408, May 2009.

[3] B. Lehman, A. Wilkins, S. Berman, M. Poplawski, and N. Johnson Miller, "Proposing measures of flicker in the low frequencies for lighting applications," in *2011 IEEE Energy Conversion Congress and Exposition*, 2011, pp. 2865–2872.

[4] A. Wilkins, J. Veitch, and B. Lehman, "LED lighting flicker and potential health concerns: IEEE standard PAR1789 update," in *2010 IEEE Energy Conversion Congress and Exposition*, 2010, pp. 171–178.

[5] T. Shimizu, T. Fujita, G. Kimura, and J. Hirose, "A unity power factor PWM rectifier with DC ripple compensation," *IEEE Trans. Ind. Electron.*, vol. 44, no. 4, pp. 447–455, 1997.

[6] T. Shimizu, Y. Jin, and G. Kimura, "DC ripple current reduction on a single-phase PWM voltage-source rectifier," *IEEE Trans. Ind. Appl.*, vol. 36, no. 5, pp. 1419–1429, 2000.

[7] P. T. Krein, R. S. Balog, and M. Mirjafari, "Minimum energy and capacitance requirements for single-phase inverters and rectifiers using a ripple port," *IEEE Trans. Power Electron.*, vol. 27, no. 11, pp. 4690–4698, Nov. 2012.

[8] S.-H. Lee, T.-P. An, and H.-J. Cha, "Mitigation of low frequency AC ripple in single-phase photovoltaic power conditioning systems," *J. power Electron.*, vol. 10, no. 3, pp. 328–333, 2010.

[9] R. S. Gemmen, "Analysis for the effect of inverter ripple current on fuel cell operating condition," *J. Fluids Eng.*, vol. 125, no. 3, p. 576, May 2003.

[10] S. B. Kjaer, J. K. Pedersen, and F. Blaabjerg, "A review of single-phase grid-connected inverters for photovoltaic modules," *IEEE Trans. Ind. Appl.*, vol. 41, no. 5, pp. 1292–1306, Sep. 2005.

[11] S. Wang, X. Ruan, K. Yao, S.-C. Tan, Y. Yang, and Z. Ye, "A flicker-free electrolytic capacitor-less AC–DC LED driver," *IEEE Trans. Power Electron.*, vol. 27, no. 11, pp. 4540–4548, Nov. 2012.

[12] G.-R. Zhu, S.-C. Tan, Y. Chen, and C. K. Tse, "Mitigation of low-frequency current ripple in fuel-cell inverter systems through waveform control," *IEEE Trans. Power Electron.*, vol. 28, no. 2, pp. 779–792, Feb. 2013.

[13] S. G. Parler, "Application guide, aluminum electrolytic capacitors." [Online]. Available: www.cornell-dubilier.com.

[14] S. K. Maddula and J. C. Balda, "Lifetime of electrolytic capacitors in regenerative induction motor drives," in *IEEE 36th Conference on Power Electronics Specialists*, 2005, pp. 153–159.

[15] H. Hu, S. Harb, N. Kutkut, I. Batarseh, and Z. J. Shen, "A review of power decoupling techniques for microinverters with three different decoupling capacitor locations in PV systems," *IEEE Trans. Power Electron.*, vol. 28, no. 6, pp. 2711–2726, Jun. 2013.

[16] The Eco Experts, "The life expectancy of solar panels." [Online]. Available: http://www.theecoexperts.co.uk/life-expectancy-solar-panels.

[17] E. D. Dunlop, "Lifetime performance of crystalline silicon PV modules," in *Photovoltaic Energy Conversion, 2003. Proceedings of 3rd World Conference on*, 2003, pp. 2927–2930.

[18] R. Wang, F. Wang, D. Boroyevich, R. Burgos, R. Lai, P. Ning, and K. Rajashekara, "A high power density single-phase PWM rectifier with active ripple energy storage," *IEEE Trans. Power Electron.*, vol. 26, no. 5, pp. 1430–1443, May 2011.

[19] S. Dusmez and A. Khaligh, "Generalized Technique of Compensating Low-Frequency Component of Load Current With a Parallel Bidirectional DC/DC Converter," *IEEE Trans. Power Electron.*, vol. 29, no. 11, pp. 5892–5904, Nov. 2014.

[20] L. Palma, "An active power filter for low frequency ripple current reduction in fuel cell applications," *Speedam 2010*, pp. 1308–1313, Jun. 2010.

[21] R.-J. Wai and C.-Y. Lin, "Development of active low-frequency current ripple control for clean-energy power conditioner," in *2010 5th IEEE Conference on Industrial Electronics and Applications*, 2010, pp. 695–700.

[22] R.-J. Wai and C.-Y. Lin, "Active low-frequency ripple control for clean-energy power-conditioning mechanism," *IEEE Trans. Ind. Electron.*, vol. 57, no. 11, pp. 3780–3792, Nov. 2010.

[23] W. Cai, B. Liu, S. Duan, and L. Jiang, "An Active Low-Frequency Ripple Control Method Based on the Virtual Capacitor Concept for BIPV Systems," *IEEE Trans. Power Electron.*, vol. 29, no. 4, pp. 1733–1745, Apr. 2014.

[24] Y. Tang, F. Blaabjerg, P. C. Loh, C. Jin, and P. Wang, "Decoupling of fluctuating power in single-phase systems through a symmetrical half-bridge circuit," *IEEE Trans. Power Electron.*, vol. 30, no. 4, pp. 1855–1865, Apr. 2015.

[25] Y. Yang, X. Ruan, L. Zhang, J. He, and Z. Ye, "Feed-forward scheme for an electrolytic capacitor-less AC/DC LED driver to reduce output current ripple," *IEEE Trans. Power Electron.*, vol. 29, no. 10, pp. 5508–5517, Oct. 2014.

[26] Y. Tang, Z. Qin, F. Blaabjerg, and P. C. Loh, "A dual voltage control strategy for single-phase PWM converters with power decoupling function," *IEEE Trans. Power Electron.*, vol. PP, no. 99, pp. 1–1, 2014.

[27] M. Chen, Y. Ni, C. M. Serrano, B. J. Montgomery, D. J. Perreault, and K. K. Afridi, "An electrolytic-free offline LED driver with a ceramic-capacitor-based compact SSC energy buffer," in *Proceedings*

of the IEEE Energy Conversion Congress and Exposition (ECCE), 2014.

[28] S. A. Khajehoddin, M. Karimi-Ghartemani, P. K.Jain, and Alireza Bakhshai, "DC-bus design and control for a single-phase grid-connected renewable converter with a small energy storage component," *IEEE Trans. Power Electron.*, vol. 28, no. 7, pp. 3245–3254, Jul. 2013.